

## Structural models and vibrational spectra of tetrahedral chalcogenide crystals and glasses

J. A. Aronovitz,\* J. R. Banavar, M. A. Marcus, and J. C. Phillips

*Bell Laboratories, Murray Hill, New Jersey 07974*

(Received 24 January 1983)

Cluster models of  $\text{Ge}(\text{S},\text{Se})_2$  containing 60 or 132 atoms were constructed. The vibrational spectra of these clusters were calculated and examined in detail in the region of the  $A_1$  (symmetric breathing) mode. Comparison with experiment shows generally good agreement and permits detailed analysis of the Raman spectra of the crystals, the compound glasses, and the alloys of  $\text{GeS}_2$  and  $\text{GeSe}_2$ .

## I. INTRODUCTION

Infrared and Raman spectroscopy are among the most powerful tools for studying the structure of disordered-network solids.<sup>1,2</sup> In general the observed spectra are broad and not easily interpreted. In the case of the tetrahedral compounds  $\text{Ge}(\text{S},\text{Se})_2$ , however, several narrow lines have been observed in the glass whose frequencies scale with and correspond closely to the normal modes of vibration of the gas-phase molecules  $\text{Ge}(\text{Cl},\text{Br})_4$ , respectively.<sup>3</sup> The relative simplicity of these spectra can be explained by the geometry of the chalcogen corner-sharing angle of  $100^\circ$ . Because this angle is close to  $90^\circ$ , the tetrahedral normal modes are largely decoupled in the glass,<sup>4</sup> producing the observed narrow lines.

Recently Bridenbaugh *et al.*<sup>5</sup> measured the Raman spectra of *c*- $\text{GeSe}_2$  and used it to analyze the spectra of *g*- $\text{GeSe}_2$ . They confirmed the previously established correspondence between the tetrahedral normal modes (symmetry labels  $A_1, E, F_2$ , and  $F_2$ ) and four peaks in the Raman spectrum of *g*- $\text{GeSe}_2$ . In addition to this analysis they provided a new structural model for the mysterious fifth line at  $214 \text{ cm}^{-1}$  in the spectrum. This line is just as narrow as and second in strength only to the  $200\text{-cm}^{-1}$   $A_1$  line, and in both  $\text{GeS}_2$  and  $\text{GeSe}_2$  its frequency is about 10% greater than that of the  $A_1$  line itself. The frequency of the  $A_1$  line very nearly scales with  $(m_c)^{-1/2}$ , where  $m_c$  is the chalcogen mass, which is what one expects because the ideal tetrahedral  $A_1$  symmetric breathing mode involves only chalcogen motion. Similar behavior for the fifth line led Bridenbaugh *et al.* to dub it "the companion  $A_1$  Raman line."

The structural origin of the companion  $A_1$  line is established by seeking a model which meets three conditions. First, as just mentioned, the mode must involve primarily chalcogen motion. Second, the mode must be associated with a large cluster. As first observed by Tronc *et al.*<sup>6</sup> and later stressed by Nemanich and Solin,<sup>7</sup> the composition dependence of the  $A_1$  line is anomalous in the  $\text{Ge}_x\text{Se}_{1-x}$  alloys, with its strength varying approximately as  $x^5$  while the ordinary tetrahedral line strength varies as  $x$  ( $0 \leq x \leq \frac{1}{3}$ ). Third, the line is very narrow,  $\Delta\nu_{1/2}/\nu \leq 0.015$ , so that it should have high symmetry and cannot really be part of some "random" network.

These conditions are very stringent and they led Bridenbaugh *et al.*<sup>5</sup> to propose that the basic structural unit in *g*- $\text{Ge}(\text{S},\text{Se})_2$  is a large cluster which is a fragment of the layer crystal structure which is still polymerized along the *a* axis but is terminated along the *b* axis by Se dimers as shown in Fig. 1. To emphasize the crucial structural role played by the Se dimers they called this partially polymerized cluster an "outrigger raft." Recently Griffiths *et al.*<sup>8</sup> have strengthened the evidence for the model substantially by showing that the rafts can be athermally annealed by Urbach-tail photons into microcrystallites. Further supporting evidence for the model has been obtained by Mössbauer spectroscopy<sup>9-11</sup> and by Urbach-photon-induced optical anisotropy (raft reorientation).<sup>12</sup>

In this paper we embark on the task of calculating the vibrational modes of these large clusters and relating them to the Raman spectra of the crystal and the glass. If we neglect layer-layer interactions there are 24 atoms in the unit cell and nearly 70  $k=0$  modes, most of which are expected to be Raman active. This is a much larger number of modes than are identifiable in the crystalline spectrum and a very much larger number than are seen in the glass. Evidently the Raman scattering strength varies enormously from one nominally Raman-active mode to another. The complexity of this situation suggests that we focus our attention on the spectral region dominated by the  $A_1$ -like normal modes which are narrow and strong. Here we still expect to find approximately eight  $A_1$ -like modes (i.e.,  $\frac{70}{9}$ ) in the crystalline spectrum, but only two are resolved. These two modes were previously assigned<sup>5</sup> to  $A_1$ -like modes of edge- and corner-sharing tetrahedra. To these we must add the  $A_1$ -like dimer modes of the glass clusters. Other possible candidates are  $A_1$ -like ring modes which were previously proposed<sup>7</sup> to explain the companion line in the glass. We find that these ring modes are present in both the crystalline unit cell and the glass clusters, but their frequencies and their polarization amplitudes render them unsuitable candidates for any of the resolved lines.

## II. MECHANICAL MODEL

## A. Force constants

A four-force-constant model was used to describe interatomic forces. Valence force fields were used rather

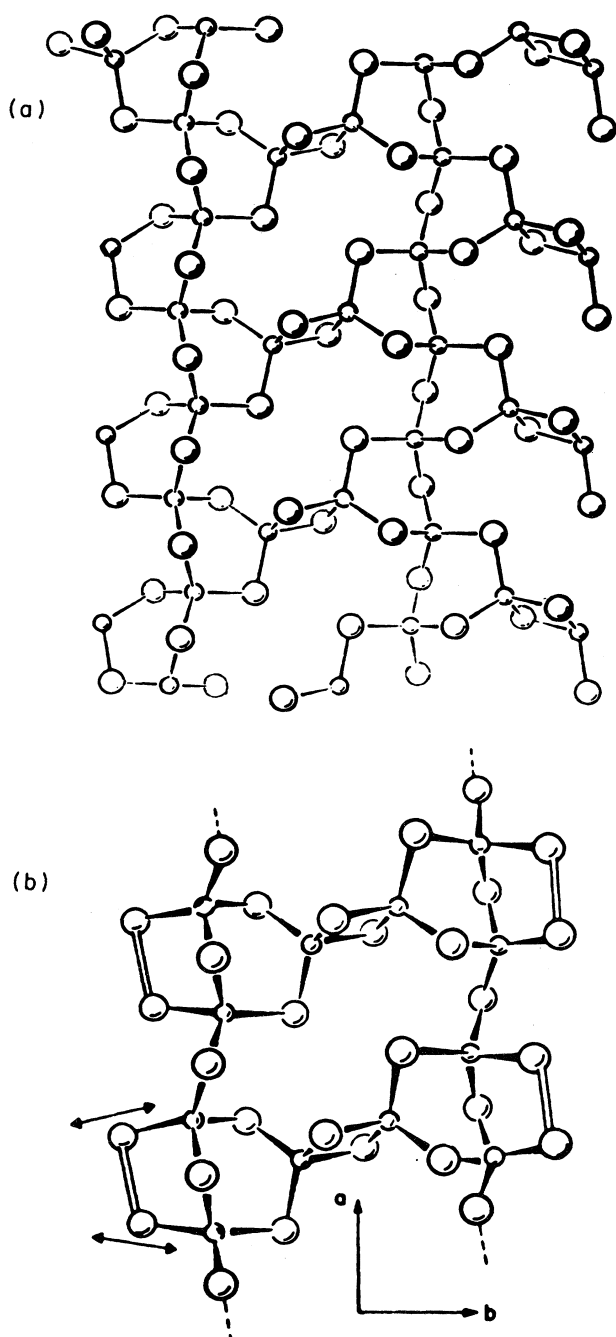


FIG. 1. Partially polymerized cluster proposed in Ref. 5 as the dominant structural unit in  $g\text{-GeS}_2$  and  $g\text{-GeSe}_2$  has an interior structure which resembles the crystal structure of  $c\text{-GeSe}_2$  [shown in (a)] while the edges parallel to the  $a$ -axis are reconstructed as shown in (b) with chalcogen dimers. Cluster model shown here, called a dimerized raft, has two  $a$ -axis chains and one set of crosslinking edge-sharing tetrahedra. Similar models with  $2n$   $a$ -axis chains and  $2n - 1$  sets of edge-sharing tetrahedra can be constructed. On the basis of Mössbauer spectra it has been suggested in Ref. 10 that  $n = 3$ , i.e., the average cluster contains six chains. While this specifies the average  $b$ -axis dimension of the cluster, the average  $a$ -axis dimension and the reconstructive mechanism which terminates the  $a$ -axis chains are at present unknown.

than central forces in order to guarantee rotational and translational invariance. This resulted in vibrational spectra which always contained four zeros, consistent with uniaxial periodic boundary conditions. The bond-stretching force constant for Ge—Se (denoted by  $k_r$ ) and the bond-bending force constant Se—Ge—Se (denoted by  $k_\theta$ ) were taken from the force constants<sup>13</sup> of  $\text{GeBr}_4$  with  $k_r$  scaled by a factor 0.85 to account for the difference<sup>14</sup> in core charge between Br and Se,

$$k_r = 2.20 \times 10^5, \quad (1)$$

in dyn/cm, and

$$k_\theta = 0.47 \times 10^5, \quad (2)$$

in  $\text{dyn}\text{\AA}^2/\text{cm}$ . Finally, we guessed a value for  $k_c$ , the Ge—Se—Ge corner- or chalcogen-centered bond-bending force constant, of

$$k_c = 0.37 \times 10^5, \quad (3)$$

in  $\text{dyn}\text{\AA}^2/\text{cm}$ . As it turned out, these force constants gave a satisfactory spectrum in reasonable correspondence with experiment. While the parameters could have been adjusted further to improve agreement with the strongest features, we did not do so. Instead we studied the dependence of the spectrum  $N(\omega)$  as a whole on the force constants, i.e.,  $d \ln \omega^2 / d \ln k$ , and these results are reported below.

The fourth force constant is  $K_r$ , the bond-stretching force constant for Se—Se. Again the difference in core charges suggests

$$K_r = \alpha k_r, \quad (4)$$

with  $\alpha = \frac{6}{4} = 1.5$ . We also tried  $\alpha = 1$  and found, because of the previously assumed<sup>5</sup> dimer geometry, that in the  $A_1$  region the dimer mode frequency was altered by only 1% between these two values. This is because the dimer breathing motion scarcely changes the dimer bond length.

### B. Cluster geometry

The cluster shown in Fig. 1 contains two corner-sharing  $a$ -axis chains which we refer to as "chains" and two sets of edge-sharing tetrahedra which crosslink the chains. In our calculations we used both two-chain and four-chain rafts each containing three sets of edge-sharing tetrahedra which are connected periodically along the  $a$  axis. These structures contain 60 and 132 atoms, respectively. The clusters are large enough to permit us to identify normal modes which are internal to the cluster and resemble crystalline modes as well as modes which are localized near the cluster edges (dimer-based modes). These large clusters also are suitable for isotopic substitution, i.e., for replacement of Se atoms by S atoms. Because the clusters are large, S-S interactions due to  $a$ -axis periodicity are relatively weak.

The atomic coordinates of the clusters were obtained from the crystallographic determination of the layer structure,<sup>15</sup> with the exception of the chalcogen-edge dimers.

These positions were determined by removing Ge atoms at the edge and rebonding the nearby Se atoms in such a manner as to give a Se—Se bond length of 2.3 Å (as in crystalline Se). With the same coordinate convention as employed by Dittmar and Schaffer<sup>15</sup> in their Table II, representative  $(x,y,z)$  coordinates of a Se dimer are (0.588,0.196,0.174) and (0.257,0.238,0.176). As mentioned above, none of our results in the  $A_1$  region are sensitive to  $K_r$ , the Se-Se force constant, although a large frequency change of the magnitude expected for the upper  $F_2$  tetrahedral normal mode<sup>16</sup> involving Se—Se bond stretching is observed in a mode split off from the 300-cm<sup>-1</sup>  $F_2$ -like band. We therefore believe that the geometry that we have used is consistent with the phenomenology developed previously.<sup>5</sup>

### III. RESULTS FOR GeSe<sub>2</sub>

The overall vibrational spectrum given by our model is shown in Fig. 2. There is a broad low-frequency band corresponding to the  $E$  and  $F_2$  bending modes between 0 and 140 cm<sup>-1</sup>, a narrow  $A_1$ -like band between 215 and 240 cm<sup>-1</sup>, and an  $F_2$ -like band between 310 and 410 cm<sup>-1</sup>. This corresponds to experimental Raman spectra<sup>5</sup> between 0 and 120 cm<sup>-1</sup>, 200 and 230 cm<sup>-1</sup>, and 280 and 320 cm<sup>-1</sup>. The crystalline spectrum also contains a weak band near 250 cm<sup>-1</sup> which does not appear in our model. This band may be due to defects in the crystal. Similar defects are probably present in cluster interiors in the glass. Overall the correspondence between our calculated

bands and the experimental bands<sup>5</sup> is quite satisfactory.

Rather than adjust the force constants to "improve" the spectrum, we examined its sensitivity to  $k_r$ ,  $k_\theta$ , and  $k_c$ . We varied these parameters over a range of as large as a factor of 3 for  $k_\theta$ , for example. We found that varying  $k_r$  changed the scale for the overall spectrum, while variations in  $k_\theta$  and  $k_c$  changed the widths of the bands. The ratio of the average  $A_1$  frequency to the average upper  $F_2$  frequency remained constant to within 10% for all our parameter variations. The narrowest bands were obtained when  $k_\theta/k_r$  was close to the value found in GeBr<sub>4</sub> and this ratio was therefore not only physically plausible but also computationally convenient.

To explore further the force-constant dependence of the spectrum, we used first-order perturbation theory to calculate  $d \ln \omega^2 / d \ln k_i$  for  $k_i = k_r, k_\theta$ , and  $k_c$ . Because  $\omega^2$  is linear in  $k$  we have

$$\sum_i \frac{d \ln \omega^2}{d \ln k_i} = 1. \quad (4)$$

In Fig. 3 we plot  $d \ln \omega^2 / d \ln k_i$  and find a somewhat unexpected result. Especially for  $k_i = k_r$  and  $k_\theta$ , the derivatives resemble step functions which are nearly constant for  $\omega \leq 200$  cm<sup>-1</sup>. In general  $d \ln \omega^2 / d \ln k_c$  is small, showing that the tetrahedral vibrations are indeed weakly coupled for geometrical reasons. This does not mean that the corner-sharing forces are weak, however, for the corner-sharing bond angle is fixed near 100° in the observed crystallographic structure, and this is almost the same value as

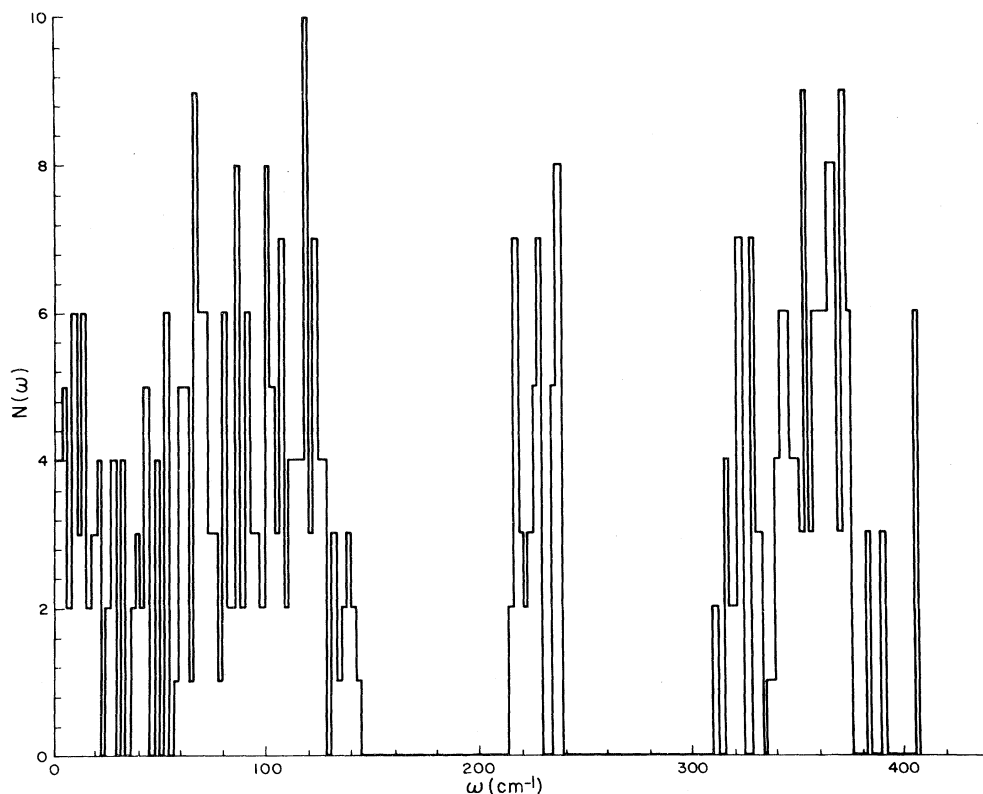


FIG. 2. Phonon spectral density  $N(\omega)$  plotted against phonon frequency  $\omega$  for the 132-atom cluster.  $A_1$ -like band is isolated from the other bands, is comparatively narrow, and is centered near 220 cm<sup>-1</sup>.

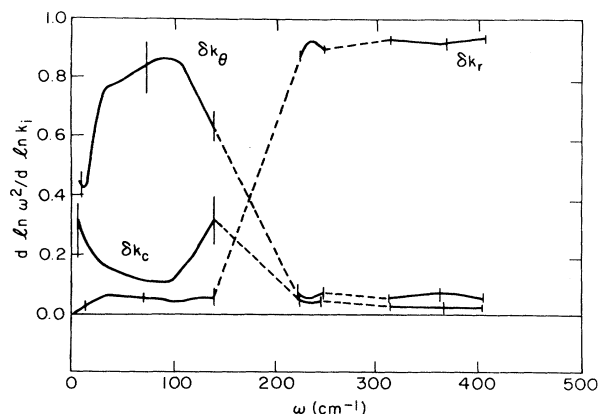


FIG. 3. Effect of varying the force constant  $k_i$  ( $=k_r, k_\theta, k_c$ ) on  $\omega$  as a function of  $\omega$ . Original digital form of this plot has been smoothed and the extent of the scatter (which is small) is indicated by the error bars. Note the well-defined separation of bending modes ( $\omega < 200 \text{ cm}^{-1}$ ) from stretching modes ( $\omega > 200 \text{ cm}^{-1}$ ) which is reflected in  $d \ln \omega^2 / d \ln k_r$ .

is observed for the spiral chains in *c*-Se. From Fig. 3 we see that the bands below  $200 \text{ cm}^{-1}$  are bending  $E$  and lower  $F_2$  modes, while those above  $200 \text{ cm}^{-1}$  depend primarily on  $k_r$ .

The next step in the analysis is to attempt to assign a Raman scattering strength to each mode. One way to do this is to introduce bond polarizabilities associated with bond stretching and bending.<sup>17</sup> Because of the high symmetry of our structure we preferred to inspect the eigen-

modes visually using three-dimensional color graphics in various perspectives. We supplemented the visual analysis with weighted histograms emphasizing the motions of dimers, and corner- and edge-sharing chalcogens. We found that visual inspection of the eigenmodes was most informative because in this way we were able to identify most directly modes corresponding to  $\vec{k}=0$  in the crystal. These modes were expected to be the only ones capable of having large Raman scattering strength not only in the crystal but in the glassy clusters as well.

Perhaps the most surprising result of our eigenmode inspection was the discovery that most of the  $\vec{k}=0$  modes in the  $A_1$  range (which was the only range we inspected in detail) are extremely well localized either on the dimer-containing edge chains, on individual interior chains or on edge-sharing tetrahedra, as shown in Fig. 4. However, viewed from the perspective of a particular tetrahedron not all the modes in the  $A_1$  range had pure  $A_1$  (symmetric breathing) character. Instead a large admixture of  $E$  (degenerate bending) character was found. If the Raman scattering strength is associated primarily with bond stretching, the  $A_1$  part of these modes is expected to make the largest contribution to the Raman scattering strength.

Our second result from the inspection of eigenmodes was that all the  $\vec{k}=0$  modes that have a large amount of  $A_1$  character are concentrated at the upper end of the  $A_1$  band. There are two distinct classes of such modes and they are illustrated in Fig. 4. Each mode in the first class ( $\omega = 235.4 \text{ cm}^{-1}$ , labeled II in Fig. 4) is localized on a specific chain or *a*-axis chain of corner-sharing tetrahedra. Alternating tetrahedra in the chain execute nearly ideal

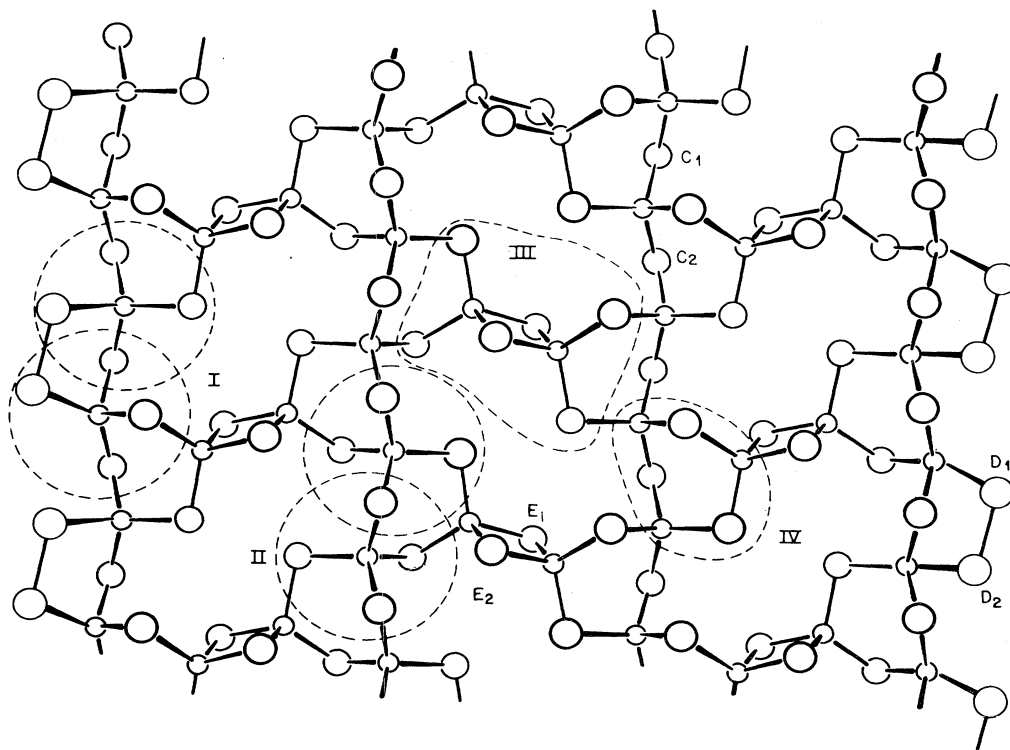


FIG. 4. Our four-chain model is shown together with selected regions ( $C$  for corner-sharing chain chalcogens,  $D$  for dimers, and  $E$  for edge-sharing chalcogens) where localized vibrational  $A_1$ -like modes are found.

$A_1$ -like motion, while the remaining tetrahedra in the chain move in almost pure  $E$ -like modes. The  $A_1$ -like frequency of the outer chains in this class (labeled I in Fig. 4) is shifted down in frequency by  $0.8 \text{ cm}^{-1}$  (relative to inner chains) by the "softness" of the dimers. The second type of mode ( $\omega = 238.3 \text{ cm}^{-1}$ , labeled III in Fig. 4) involves primarily the symmetric breathing of the outer four (corner-sharing) chalcogens of an edge-sharing bi-tetrahedral unit which crosslinks the  $a$ -axis chains. Close examination shows, however, that the individual chalcogens in this partially clamped mode do not move in so nearly an  $A_1$ -like mode as some of the tetrahedra do in the  $a$ -axis chains. This reduction in  $A_1$ -like symmetry may explain the tenfold reduction in Raman scattering strength observed<sup>5</sup> in the crystal for the upper  $A_1$  peak compared to the lower one. The large disparity in Raman scattering strengths has previously been used<sup>5</sup> to assign the peaks to edge- and corner-sharing tetrahedra, respectively. Moreover, our computed (edge-sharing)–(corner-sharing)  $A_1$ -like splitting of  $+3 \text{ cm}^{-1}$  has the right sign and its magnitude agrees well with that observed<sup>5</sup> in the crystal ( $5 \text{ cm}^{-1}$ ).

In our calculations we assumed that  $k_\theta$  and  $k_c$  were independent of bond angle, whereas we would actually expect the chalcogen-centered bending forces in the four-membered edge-sharing rings (chalcogen bond angle of  $80^\circ$ ) to be substantially larger than those for the six-membered corner-sharing rings (chalcogen bond angle of  $100^\circ$ ). Increasing the edge-sharing frequency by 1% ( $2 \text{ cm}^{-1}$ ) to give the  $5\text{-cm}^{-1}$  splitting is equivalent, according to Fig. 3, to strengthening  $k_\theta + k_c$  (edge) by about 40%. This is reasonable, since the edge-sharing bond angles are about  $20^\circ$  smaller than the corner-sharing ones.<sup>15</sup> Our calculations show that the outer chain mode, which is our candidate for the "companion"  $A_1$  mode, lies about  $0.8 \text{ cm}^{-1}$  lower than the  $A_1$  mode derived from the crystalline mode. At first we were disappointed by this result, as the  $A_1$ -companion  $A_1$  experimental splitting observed in the glass is  $+14 \text{ cm}^{-1}$  (or  $+17 \text{ cm}^{-1}$  when scaled to our  $A_1$  frequency of  $235 \text{ cm}^{-1}$ ). However, we have concluded that for isolated fragments it is entirely reasonable that the edge modes should have lower frequency. In the physical glass, of course, there must be strong cluster-cluster interactions which are responsible for the cohesion of the material but which are omitted from our model. We can use the observed shift to estimate the strength of these perturbations.

To make such an estimate, we note that both the  $A_1$  and companion  $A_1$  lines are broadened in the glass by about  $15 \text{ cm}^{-1}$  full width at half-maximum (FWHM), i.e., the broadening is nearly equal to the ( $A_1$ -companion)–( $A_1$ ) splitting  $\gamma$ . This suggests that the effects which are external to the cluster, as measured (in  $\text{cm}^{-1}$ ) by  $\Gamma$  or by an effective external force constant proportional to  $\Gamma^2$ , are incoherent with the internal cluster forces, i.e.,

$$\Gamma^2 = (200 + \gamma)^2 - (200)^2 \approx 400\gamma, \quad (5)$$

$$\Gamma = 76, \quad (6)$$

the latter in  $\text{cm}^{-1}$ .

We can infer from Eq. (6) something about the nature

of the intercluster interactions. The van der Waals forces associated with the sliding of layer against layer<sup>5</sup> give interlayer frequencies of  $17$  and  $30 \text{ cm}^{-1}$ , much smaller than  $\Gamma$ . On the other hand, the lowest tetrahedral bending mode, the  $E$  mode, has a frequency of  $80 \text{ cm}^{-1}$ , very close to  $\Gamma$ . We conclude that the clusters are so strongly associated that the dimer modes at the edge are deformed on a one- $E$ -phonon scale. This is a consistent picture because only  $n=1$  phonons are involved, which implies that the splitting  $\gamma$  and the widths of the  $A_1$  and companion modes should be nearly equal, as they are indeed observed to be, with fluctuations of order  $\sqrt{n} = 1$  as well. Considering the inevitable complexity of cluster-cluster interactions we are more than satisfied with this description.

#### IV. ISOTOPIC SUBSTITUTION

The Raman spectra of  $\text{Ge}(\text{S}_x\text{Se}_{1-x})_2$  glasses for  $x = n/32$  ( $n = 1, 2, 4, 8$ ) have been studied recently<sup>14</sup> in an effort to use the isotopic substitution as a probe of the glass structure and the phenomenon of athermal laser annealing. In the isotopically analogous molecules  $\text{GeCl}_m\text{Br}_{4-m}$  quasi- $A_1$  modes are observed<sup>13</sup> to shift nearly linearly in frequency for  $n = 0-3$ . It was therefore not surprising to find nearly linearly shifted mixed-tetrahedral  $A_1$  peaks in the glass, and a simple phenomenological broken-symmetry model was used to describe the glass spectra.<sup>14</sup>

In order to study this question further we have calculated perturbed vibrational spectra with  $m_{\text{Se}}$  replaced by  $m_{\text{S}}$  on one or two sites of a given tetrahedron. (We assumed, in accordance with conventional size-electronegativity parameters, that the chemical changes in Ge-S compared to Ge-Se force constants were negligible.) The simplest cases involve one substitution or pairs of substitutions at the equivalent sites  $C_1C_2$ ,  $D_1D_2$ , and  $E_1E_2$  as shown in Fig. 4. With  $m_{\text{Se}}/m_{\text{S}} = 2.5$  the dominant effects of the chemical substitution are described by the mass change which is large compared to the chemical changes in the force constants (e.g., S and Se have nearly equal Pauling electronegativities).

Our results show that in most cases even with only one mass substitution more than one mode is pushed above the  $A_1$  band. Usually the modes pushed out are well separated in frequency. The higher-frequency impurity mode always has more  $A_1$  character while the lower one has more  $E$  character, reflecting the mixed  $A_1-E$  symmetry of the parent quasi- $A_1$  band as previously discussed, and the large value of the mass perturbation. In Table I we summarize the higher-(more  $A_1$ -like) frequency shifts for sites mentioned above.

TABLE I. Trends in isotopically split  $\text{Ge}(\text{S}_n\text{Se}_{4-n})_{1/2}$  tetrahedral  $A_1$ -like reduced multiplet frequencies  $\Delta\omega(n)/\omega_1(0)$ , where  $\Delta\omega(n) = \omega(n) - \omega(n-1)$ . Experimental value of  $0.07$  for  $\Delta\omega_1(1,2)/\omega_1(0)$  is in good agreement with our calculated values for the  $C$  sites.

	Dimer	C	Edge
$\Delta\omega(1)/\omega_1(0)$	0.08	0.06	0.11
$\Delta\omega(2)/\omega_1(0)$	0.02	0.08	0.11

The linearity, i.e.,  $\Delta\omega(1)=\Delta\omega(2)$ , found experimentally is absent for the dimer modes apparently because of severe breakdown in tetrahedral character for the pair-substituted case. Both corner- and edge-sharing pairs retain the linearity observed in the free-gas multiplets. However, the numerical agreement between the experimental values  $\Delta\omega(1)$  and  $\Delta\omega(2)=0.07$  and the calculated values are much better for the  $C_1C_2$  pair, and we therefore conclude that S substitution occurs preferentially on C-type sites.

With the benefit of hindsight we can also argue that the C sites should be preferred to edge sites or dimerized sites for replacement of Se by S. The respective cohesive energies of c-S and c-Se are 67 and 54 kcal/mole,<sup>18</sup> corresponding to an enthalpy difference of 0.6 eV/bond. Thus S will avoid highly strained sites such as the edge-sharing and dimerized sites and will prefer the C sites where all bond angles are close to their ideal values.

### V. CONCLUSIONS

In general the vibrational spectra of noncrystalline solids are broad and difficult to interpret. In this paper we have shown that the quasi- $A_1$  region of the Raman spectrum of g-GeSe<sub>2</sub> is exceptionally simple for a disordered solid and interpretable in remarkably quantitative detail. Our calculations show that this simplicity stems from the combined effects of the following factors.

(1) The fundamental building block in the glass is the tetrahedron. The  $A_1$  (symmetric breathing) mode of these tetrahedra generates a narrow band ( $\Delta\omega/\omega_1 \lesssim 0.15$ ) of vibrational modes which is well separated from the remaining bands in both the crystal and the glass.

(2) Within this narrow band of vibrational modes the Raman-active modes in the crystal form an even narrower band ( $\delta\omega/\omega_1 \lesssim 0.02$ ). Our calculated values of  $\delta\omega$  are in good agreement with experiment for c-GeSe<sub>2</sub>.

(3) The breadth of the  $A_1$  band in the glass is increased to  $\gamma/\omega_1 \sim 0.08$ , which we explain in terms of cluster-cluster interactions. We suggest, furthermore, that the same interactions can explain the splitting of the interior (*a*-axis chain) Raman  $A_1$  mode and the companion (dimer and edge *a*-axis chain) Raman modes. The strength of these interactions suggests strong association of cluster

edges (e.g., to partially polymerized ethanelike clusters) as proposed previously.<sup>8</sup>

(4) The previously observed<sup>14</sup> linear multiplet ladder of  $A_1$  modes in isotopically mixed  $\text{Ge}(\text{S}_n\text{Se}_{4-n})_{1/2}$  tetrahedra can be explained qualitatively and quantitatively in terms of substitution at preferred *a*-axis chain sites. Other sites do not produce as good agreement with experiment. It appears that the high symmetry of the *a*-axis chains plays an important role in achieving this agreement. Without this symmetry we see no reason to expect to find either a narrow  $A_1$  line or narrow isotopically shifted images of the  $A_1$  line.

*Note added.* After completion of the present work we received an unpublished manuscript describing Japanese work which had reached similar conclusions.<sup>19</sup> This work contains one specific feature not included in our text, that is, these authors identify our crystalline defect line at 247 (443)  $\text{cm}^{-1}$  in GeSe<sub>2</sub> (GeS<sub>2</sub>) as the signature of a Se—Se (S—S) stretch mode of a Se (S) dimer embedded in a crystalline or quasicrystalline GeSe<sub>2</sub> (GeS<sub>2</sub>) cluster. We are impressed by the cogency of the evidence for this assignment put forward by these authors and generally support their interpretation. After this paper was submitted strong circumstantial support for our treatment of cluster-cluster interactions [see Eqs. (5) and (6)] was obtained experimentally by Magaña and Lannin.<sup>20</sup> They found that both the  $A_1$  band near 200  $\text{cm}^{-1}$  and the  $A_{1c}$  band near 220  $\text{cm}^{-1}$  are still present in liquid GeSe<sub>2</sub> and that while the relaxation of atomic interactions at higher temperatures in the liquid lowers the  $A_1$  frequency by 3%, the  $A_{1c}$  frequency is lowered by 5%. The additional 2% reduction of the  $A_{1c}$  frequency is explained in our model as a 10% reduction in  $\gamma$ , or a 5% reduction in  $\Gamma$ , the parameters which describe cluster-cluster interactions. These figures seem eminently reasonable—small and certainly of the right sign—to describe reduced cluster-cluster interactions in the liquid compared to the glass.

### ACKNOWLEDGMENTS

We are grateful to J. E. Griffiths for informative discussions and to B. C. Chambers and A. L. Simons for their unlimited patience.

\*Present address: Physics Department, Harvard University, Cambridge, Mass. 02138.

<sup>1</sup>J. Wong and C. A. Angell, *Glass: Structure by Spectroscopy* (Dekker, New York, 1976).

<sup>2</sup>J. C. Phillips, *Phys. Today* **34**(2), 1 (1982).

<sup>3</sup>N. Kumagai, J. Shirafuji, and Y. Inuishi, *J. Phys. Soc. Jpn.* **42**, 1261 (1977).

<sup>4</sup>M. F. Thorpe, in *Vibrational Spectroscopy of Molecular Liquids and Solids*, edited by S. Bratos and R. M. Pick (Plenum, New York, 1979), p. 341.

<sup>5</sup>P. M. Bridenbaugh, G. P. Espinosa, J. E. Griffiths, J. C. Phillips, and J. P. Remeika, *Phys. Rev. B* **20**, 4140 (1979).

<sup>6</sup>P. Tronc, M. Bensoussan, A. Brenac, and C. Sebenne, *Phys. Rev. B* **8**, 5947 (1973).

<sup>7</sup>R. J. Nemanich and S. A. Solin, *Solid State Commun.* **21**, 273 (1977); R. J. Nemanich, *Phys. Rev. B* **16**, 1655 (1977).

<sup>8</sup>J. E. Griffiths, G. P. Espinosa, J. P. Remeika, and J. C. Phillips, *Solid State Commun.* **40**, 1077 (1981); *Phys. Rev. B* **25**, 1272 (1982).

<sup>9</sup>W. J. Bresser, P. Boolchand, P. Suranyi, and J. P. de Neufville, *Phys. Rev. Lett.* **46**, 1689 (1981).

<sup>10</sup>P. Boolchand, W. J. Bresser, and M. Tenhover, *Phys. Rev. B* **25**, 2971 (1982).

<sup>11</sup>P. Boolchand, J. Grothaus, W. J. Bresser, and P. Suranyi, *Phys. Rev. B* **25**, 2975 (1982).

<sup>12</sup>J. Hajt6, I. Jánossy, and G. Forgács, *J. Phys. C* **15**, 6293 (1982).

<sup>13</sup>C. Cerf and M. B. Delhaye, *Bull. Soc. Chim. Fr.* **1964**, 2818;

- C. Cerf, *ibid.* 1971, 2889.
- <sup>14</sup>J. E. Griffiths, J. C. Phillips, G. P. Espinosa, and J. P. Remeika, *Phys. Rev. B* 26, 3499 (1982).
- <sup>15</sup>G. Dittmar and H. Schaffer, *Acta Crystallogr. Sect. B* 12, 1188 (1976); 12, 2276 (1976). These papers include tables of bond lengths and bond angles which can be used to quantify our qualitative descriptions of the strains arising from tetrahedra sharing edges, etc.
- <sup>16</sup>E. B. Wilson, Jr., J. C. Decius, and P. C. Cross, *Molecular Vibrations* (McGraw-Hill, New York, 1955) p. 175.
- <sup>17</sup>R. J. Bell and D. C. Hibbins-Butler, *J. Phys. C* 9, 2955 (1976).
- <sup>18</sup>D. D. Wagman *et al.*, National Bureau of Standards Technical Note 270-3 (unpublished). Available from U. S. G.P.O., Washington, D.C.
- <sup>19</sup>K. Murase, T. Fukunaga, Y. Tanaka, K. Yakushiji, and I. Yunoki, in *Proceedings of the International Conference on Semiconductors, 1982*, edited by M. Averous (North-Holland, Amsterdam, 1983), p. 962.
- <sup>20</sup>J. R. Magaña and J. S. Lannin, *Bull. Am. Phys. Soc.* 28, 328 (1983).